The Canadian Mineralogist
Vol. 39, pp. 1617-1633 (2001)

QUANTITATIVE PHASE-ANALYSIS BY THE RIETVELD METHOD USING X-RAY POWDER-DIFFRACTION DATA: APPLICATION TO THE STUDY OF ALTERATION HALOS ASSOCIATED WITH VOLCANIC-ROCK-HOSTED MASSIVE SULFIDE DEPOSITS

THOMAS MONECKE[§], SIBYLLE KÖHLER, REINHARD KLEEBERG AND PETER M. HERZIG

Institute of Mineralogy, Freiberg University of Mining and Technology, Brennhausgasse 14, D-09596 Freiberg, Germany

J. BRUCE GEMMELL

Centre for Ore Deposit Research, School of Earth Sciences, University of Tasmania, GPO Box 252-79, Hobart, Tasmania 7001, Australia

ABSTRACT

Quantitative determination of the mineralogical composition of hydrothermally altered rocks was performed by means of the Rietveld method using X-ray powder-diffraction data. Initially, experiments were carried out to minimize systematic errors arising from preferred orientation of particles as well as micro-absorption. The precision of the proposed method was tested by independent replicate sample-preparation and analyses. The closeness of the replicate phase-determinations showed that random within-laboratory errors were comparatively small. Expressed as chemical compositions, the quantitative results are in good agreement with the major oxide concentrations determined by X-ray fluorescence. The results indicate that the relative abundances of phases and refined element substitutions were accurately determined. The method developed was applied to hydrothermally altered rocks from the Waterloo volcanic-rock-hosted massive sulfide (VHMS) deposit in Queensland, Australia. Hierarchical cluster analysis led to the discrimination of several mineralogically distinct alteration-induced assemblages. These mineral assemblages are characteristic of specific zones of alteration. The strong spatial zoning with respect to the mineralized body and the distinct mineralogical assemblages of the alteration halo are interpreted to result primarily from varying degrees of hydrolytic decomposition and potassium metasomatism of the wallrocks. Based on these results, we suggest that quantitative phase-analysis by the proposed method represents a new powerful tool in studies of alteration halos.

Keywords: quantitative phase-analysis, Rietveld method, alteration mineralogy, volcanic-rock-hosted massive sulfide deposits, Waterloo VHMS deposit, Queensland, Australia.

SOMMAIRE

Nous avons pu déterminer de façon quantitative la composition minéralogique de roches sujettes à une altération hydrothermale au moyen d'une analyse selon la méthode de Rietveld de traitement de données de diffraction X obtenues sur poudre. Au départ, les expériences ont porté sur une minimisation des erreurs systématiques dues à l'orientation préférentielle des particules et à la micro-absorption. La précision de notre méthode a pu être vérifiée par préparations et analyses répétées des échantillons. La concordance des résultats répétés portant sur la détermination des phases montre que les erreurs aléatoires intra-laboratoire sont relativement petites. Exprimées en termes de compositions chimiques, les résultats quantitatifs concordent bien avec la proportion des éléments majeurs tels qu'établie par fluorescence X. Les résultats indiquent que les abondances relatives des phases et les schémas de substitutions d'éléments sont affinés avec justesse. Nous avons appliqué la méthode aux roches volcaniques altérées par voie hydrothermale au gisement de sulfures massifs de Waterloo, au Queensland, en Australie. Une analyse par groupements hiérarchique mène à la discrimination de plusieurs assemblages minéralogiques attribuables à l'altération hydrothermale. Ces assemblages sont caractéristiques de zones spécifiques réparties autour du gisement, et résulteraient surtout d'une altération plus-ou-moins avancée menant à la déstabilisation hydrolytique et à la métasomatose potassique. A la lumière de ces résultats, nous croyons que l'analyse quantitative des phases selon la démarche proposée fournit un outil nouveau et puissant dans l'étude des auréoles d'altération.

(Traduit par la Rédaction)

Mots-clés: analyse quantitative des phases, méthode de Rietveld, minéralogie des zones d'altération, gisements de sulfures massifs, encaissant volcanique, gisement de Waterloo de type VHMS, Queensland, Australie.

§ *E-mail address:* tmonecke@mineral.tu-freiberg.de

Introduction

Over the past decades, much work has been conducted in and around volcanic-rock-hosted massive sulfide (VHMS) deposits to determine the effects of alteration on the mineralogical, geochemical, and isotopic characteristics of the wallrocks (Franklin *et al.* 1981, Urabe & Scott 1983, Richards *et al.* 1989, Marquis *et al.* 1990, Gemmell & Large 1992, Large 1992, Barrett *et al.* 1993, Leistel *et al.* 1998). However, the quantitative description of mineralogical changes during alteration has been hampered by the lack of analytical techniques allowing a correct determination of the relative abundance of minerals in the altered (and unaltered) rocks. Traditionally, the determination of the relative abundances of the constituent minerals in rocks has been carried out by (1) point-counting techniques or image analyses of thin sections, (2) normative calculations based on whole-rock geochemical data, and (3) conventional X-ray powder-diffraction (XRD) measurements using integrated peak-intensities combined with some scheme of internal or external calibration. However, the applicability of these techniques to quantitative phase-analysis of intensely altered rocks is limited owing to the very nature of these rocks. In most cases, point counting is inappropriate because hydrothermally altered rocks are very fine grained or intensely foliated. Normative calculations typically assume idealized compositions of the component minerals and may, therefore, not yield reliable estimates of the true compositions. Conventional X-ray powder-diffraction techniques using calibration curves or internal standards are also troublesome because standards with physical and chemical properties similar to the rocks investigated have to be obtained or prepared, which may be extraordinarily difficult in the case of products of hydrothermal alteration. Moreover, extensive peak-overlaps as well as the effects of preferred orientation typically prohibit a correct determination based on single-peak intensities, as required by these techniques. Some problems associated with conventional X-ray methods can be overcome by application of the Rietveld method.

Phase Analysis by the Rietveld Method

The Rietveld method is a full-profile approach that was initially introduced for the refinement of crystal-structure parameters (Rietveld 1969) but has been expanded over the last ten to fifteen years for application in quantitative phase-analysis. The method is based on a least-squares fit between step-scan data of a measured diffraction pattern and a simulated X-ray-diffraction pattern. The simulated XRD pattern is calculated from a large number of parameters, including crystal-structure parameters of each component phase, a scale factor for each constituent phase to adjust the relative intensities of the reflections, parameters describing the peak profile and the background, and parameters simulating the instrumental aberrations as well as effects resulting from size-related strain, preferred orientation, and particle size. A key feature of the quantitative analysis of phase proportions by the Rietveld method is that the phase abundances of the constituent phases can be directly calculated from the refined scale-factors. Therefore, quantitative analysis can be performed without the need of experiments undertaken on standard samples to calibrate the method (Hill & Howard 1987, Bish & Howard 1988, Snyder & Bish 1989, Bish & Post 1993, Hill *et al.* 1993, Mumme *et al.* 1996, Raudsepp *et al.* 1999, Gualtieri 2000, Guirado *et al.* 2000, Hillier 2000).

Although the Rietveld method may potentially be useful in the study of hydrothermally altered rocks, an accurate quantitative analysis is challenging because of the large number of phases contained in these rocks and their chemical and structural variability. In particular, the occurrence of layer disorder in phyllosilicates contained in the altered rocks may cause considerable difficulties in quantitative phase-analysis by the Rietveld method (Bish 1993, Hillier 2000). Moreover, the effects of preferred orientation and micro-absorption are significant problems encountered in Rietveld refinement (Bish & Reynolds 1989, Bish & Post 1993, Madsen *et al.* 2001), and systematic errors arising from these effects need to be minimized to obtain meaningful results. In the present paper, a procedure of sample preparation and analysis is described that has been designed to lead to a correct analysis of hydrothermally altered rocks. The precision and accuracy of the method were evaluated using whole-rock samples collected from the alteration halo of the Waterloo VHMS deposit, Australia. Particular efforts were undertaken to develop a procedure that can be used as a matter of routine in studies of alteration halos in VHMS-type deposits.

Geological Background and Sample Strategy

The Waterloo VHMS deposit is located in the Charters Towers region in northern Queensland. The volcanic host-rocks of the deposit belong to the Seventy Mile Range Group that forms a major east–west-trending relic of Cambro–Ordovician back-arc volcanism 165 km long at the northern end of the Tasman Fold Belt System (Henderson 1986, Berry *et al.* 1992, Stolz 1995). The mineralization at Waterloo led to a relatively small high-grade base-metal resource of 0.372 Mt at 3.8% Cu, 19.7% Zn, 2.8% Pb, 94 g/t Ag, and 2 g/t Au (Berry *et al.* 1992, Huston *et al.* 1995). The blanket-like massive sulfide bodies are underlain by an extensive footwall alteration characterized by intensely altered and schistose rocks. In the periphery of the footwall alteration halo, these intensely altered volcanic rocks grade into moderately to weakly altered andesite containing relict volcanic textures. The immediate hanging-wall to the massive sulfides is composed of coarse quartz–feldspar crystal-rich sandstone and breccia that have been intruded by a dacite cryptodome. The upper part of the

hanging wall consists of mudstone, fine sandstone, coarse feldspar–quartz sandstone and breccia, basalt, andesite, and rare dacite. The 80 whole-rock samples used in the present study were collected from exploration diamond-drill core throughout the footwall of the massive sulfides.

Experimental Methods

Sample preparation and measurement

Initially, the drill-core samples (2 kg) were crushed, and rock chips containing visible vein material were removed. A split of 300 g was subsequently pulverized in a disc mill. One part of the powder obtained was taken for X-ray fluorescence (XRF) analysis on standard fused beads and pressed pellets using a Philips automated XRF spectrometer. Preparation of the sample powder for the XRD measurement was carried out in the following manner. To avoid additional layer disorder of the phyllosilicates contained in the samples, a split of the powder (~ 1 g) was further pulverized by hand in an agate mortar, and the fine powder was stepwise removed by sieving (20 μm mesh). Subsequently, the fine powder was vibrated along with small steel balls for five minutes to achieve homogeneous mixing. The powders were then filled into conventional top-loading holders (26 mm opening diameter) using the method described below. Step-scan XRD data (5 to 80° 2θ, 0.03° 2θ step, 8 s/step) were collected with an URD 6 (Seifert–FPM, Germany) diffractometer. The diffractometer was equipped with a diffracted-beam graphite monochromator and a variable divergence slit that allowed the irradiation of a constant area of sample (355 mm^2) on the rotated sample. A Co tube was used and operated at 40 kV and 30 mA.

TABLE 1. SOURCES OF CRYSTAL-STRUCTURE DATA USED TO DERIVE STARTING STRUCTURES FOR THE QUANTITATIVE PHASE-ANALYSIS BY THE RIETVELD METHOD

Mineral	Source of crystal-structure data
Albite	Williams & Megaw (1964)
Calcite	Effenberger *et al.* (1981)
Chlorite	Rule & Bailey (1987)
Epidote	Dollase (1971)
Kaolinite	Bish & Von Dreele (1989)
Muscovite	Güven (1971)
Na–K mica‡	Comodi & Zanazzi (1995)
Paragonite	Sidorenko *et al.* (1977)
Pyrite	Brostigen & Kjekshus (1969)
Pyrophyllite	Wardle & Brindley (1972)
Quartz	Young & Post (1962)
Rutile	Meagher & Lager (1979)
Titanite	Taylor & Brown (1976)

‡ Na–K mica with Na/K values intermediate between muscovite and paragonite formed as a metastable phase during alteration (Monecke *et al.* 2000).

Rietveld refinement and quantitative phase-analysis

Qualitative phase-analysis of the raw diffraction patterns was carried out by conventional search/match procedures using reference diffraction patterns stored in the ICDD PDF–2 (International Centre for Diffraction Data). Identification of minor mineral phases in complex diffraction patterns was, therefore, limited to phases having relatively distinct peak-positions. Quantitative analysis was performed using the fundamental-parameter Rietveld refinement programs BGMN/AutoQuan (Bergmann *et al.* 1994, 1998, Taut *et al.* 1997). We have chosen this software package for several reasons, including the numerical stability and the convenient refinement in fully automatic mode without a user-defined strategy for refinement, enabling routine analysis.

Crystal-structure models

The use of the Rietveld method requires knowledge of the approximate crystal-structure of each phase present in the sample investigated. Such crystal-structure information as well as starting parameters of site occupancies and lattice parameters were taken from the literature (Table 1). In the Rietveld program used, the parameter space can be limited by the introduction of physically and mineralogically meaningful upper and lower limits for each parameter. The limitation of the parameter space substantially improves the stability of the refinement and also leads to a better convergence into the global minimum. The upper and lower limits of the crystal-structure parameters were derived experimentally by investigation of a large number of natural samples. Prior to the present study, the applicability of the starting crystal-structure models obtained and parameter limits was tested in experiments using synthetic 50:50 mineral mixtures of known compositions.

The refined crystal-structure parameters included the unit-cell parameters of each phase as well as element substitutions with pronounced influences on intensities and positions of reflections. For instance, the Mg^{2+}–Fe^{2+} occupancy of the octahedral positions in the chlorite structure was refined owing to its control on the intensity distribution of the chlorite basal reflections. Another important element substitution considered was the nature of the interlayer cation in a true dioctahedral mica because of its influence on the intensity ratios of the basal reflections of that mica.

A particular problem encountered was the disorder by $\pm b/3$ layer displacement of chlorite. This layer displacement yields (1) sharp and intense 00*l* peaks, (2) fairly sharp, but less intense *hkl* peaks with $k = 3n$, (3) extremely wide *hkl* peaks with $k \neq 3n$, and (4) broadening and minor shifts of the 0*k*0 peaks in the diffraction patterns. In order to describe these diffraction patterns correctly, a specially designed real-structure model was implemented into the starting structure of this mineral

(Bergmann & Kleeberg 1998). This real-structure model was successfully applied during refinement of diffraction patterns of samples from the Waterloo deposit that contain a high concentration of chlorite (> 10 wt.%).

Description of peak profile

The peak profiles were described by separate consideration of the wavelength distribution of the X-ray tube, the instrumental assemblage (*e.g.*, length of divergence slit, focus and length of detector slit, sample dimension and thickness), and the contribution of the phases contained in the sample (*e.g.*, crystallite sizes and degree of microstrain). During routine Rietveld analysis, only the sample function was refined because the wavelength distribution of the X-ray tube is constant and the instrumental settings remained unmodified.

In the Rietveld software used, the wavelength distribution was modeled by a set of four Lorentz functions describing the $K\alpha_1$ and $K\alpha_2$ lines of the Co tube. This model was based on the spectral measurements carried out by Hölzer *et al.* (1997). The instrumental profile function was derived by a Monte Carlo ray-tracing method prior to the Rietveld refinement (Bergmann *et al.* 1997, 1998, 2000). This simulation method includes the calculation of instrumental profile shapes at defined angular steps as well as the intensity function of the automatic divergence slits. The procedure described by Bergmann *et al.* (2000) was followed to describe the low-intensity tails occurring on both sides of all Bragg reflections, which is due to emission of X-rays outside the focus of the X-ray tube.

The sample profile function was represented by folding of a Lorentzian and a squared Lorentzian profile describing the size and microstrain broadening, respectively (Bergmann *et al.* 2000). The size broadening is independent of 2θ and was assumed to be isotropic for all phases contained in the samples. An isotropic microstrain-induced broadening parameter was only introduced in the case of albite because the width of the albite reflections varied as a function of 2θ, possibly owing to variations in the chemical composition. Moreover, microstrain-induced broadening was considered in the *hkl*-dependent broadening models for the layer silicates. Together with up to 14 parameters of the background polynomial function and the relatively large number of parameters introduced by the models of preferred orientation (see below), a total of up to 140 independent parameters was reached.

Optimization of the Experimental Method

Systematic experiments were carried out prior to routine analyses of the samples from the Waterloo deposit to optimize the methods of sample preparation and analysis. Particular efforts were undertaken to minimize and correct the effects of micro-absorption and preferred orientation.

Particle size and micro-absorption

Micro-absorption occurs in the samples because the constituent minerals have very different coefficients of linear absorption (Co$K\alpha$: quartz 146 cm^{-1} and pyrite 516 cm^{-1}). This effect results in the systematic underestimation of the highly absorbing pyrite in the quantitative phase-analysis. Although micro-absorption can be minimized by very fine grinding of the powders, overgrinding has to be avoided because excessive mechanical treatment would result in substantial layer disorder of the phyllosilicates. Therefore, the samples were carefully pulverized by hand, and the ground sample was sieved periodically during the grinding process to remove the material of small size (<20 μm). Moreover, Co$K\alpha$ radiation was used in the present study to reduce the contrast in the absorption coefficients among the minerals contained in the samples (Bish & Reynolds 1989).

To correct the effects of micro-absorption during Rietveld refinement, the mean particle-size of each constituent mineral has to be determined (Brindley 1945, Taylor & Matulis 1991). However, this is not possible because the minerals contained in the finely powdered samples cannot be readily separated. Nevertheless, mineral separation takes place to some extent during the process of sieving and grinding owing to differences in the hardness and fissility of the different minerals. In the samples investigated, powder passing the sieve at an early stage of the grinding process contains a high proportion of phyllosilicates, whereas most of the pyrite passes the sieve at the final stage. Therefore, mean particle-sizes can be estimated for these minerals by measuring the particle-size distributions of the material of small size passing the sieve at different stages of the grinding procedure.

As an example, several grams of one representative sample (WT22–163) were sieved and ground by hand, and the powder that passed the sieve was split into four subsequent fractions (F1 to F4) after approximately equal times of sieving and grinding. The first fraction that passed through the sieve (F1) contains a high percentage of phyllosilicates, whereas the last fraction (F4) has a high pyrite content. Mean particle-sizes of the four fractions, determined on a Leeds & Northrup Microtrac laser-based particle-size distribution granulometer, increase from 4 μm (F1) to 8 μm (F4). Thus, phyllosilicate particles are, in general, smaller than the pyrite particles. The mean particle-sizes were used in the Rietveld analyses of the four fractions, and their mineral modes were determined (Fig. 1). As the weights of the fractions F1 to F4 were also measured, the mineral modes of the sample WT22–163 could be calculated (Fig. 1). Sample WT22–163 was also prepared conventionally by sieving and grinding the whole powder at once. The mean particle-size of the conventionally prepared sample is 6 μm, and this value was used as a parameter for all constituent minerals in the Rietveld

analysis of this sample. For the highly absorbing pyrite, the resulting product of the mean grain-size and the linear absorption coefficient for Co$K\alpha$ yields a value of 0.3096. This value is in the lower interval of coarse powders as defined by Brindley (1945). Therefore, micro-absorption correction can be applied during Rietveld refinement. Taking the errors of the method into account (see below), Figure 1 shows that the mineral modes determined on the conventionally prepared sample are identical to the mode of the calculated composition derived from a more accurate correction of the effects of micro-absorption.

The results of the experiment suggest that the influence of micro-absorption can be minimized sufficiently if an appropriate mean particle-size of the analyzed multiphase powder is known and used as a global parameter for the grain sizes of all constituent phases. Because the method of sample preparation was similar for all samples, routine analysis was based on the assumption that the mean particle-sizes of all samples was identical (~6 μm).

Particle orientation

The second serious problem encountered was the preparation of XRD samples with minimal preferred orientation of the particles. The preparation of sample mounts with random orientation of all grains was precluded by the non-spherical shape of the grains that form during the process of milling, sieving, and grinding in response to the physical properties of the constituent minerals. Previous investigators have shown that the effects of preferred orientation can be largely minimized by collecting step-scan data on rotated glass capillaries (Hill *et al.* 1993, Mumme *et al.* 1996). However, this method of sample preparation is not convenient for routine measurements because of the time-consuming preparation of the capillaries and the long counting-times per step needed to achieve appropriate counting statistics. Moreover, the size of the capillary limits the amount of powder analyzed and small inhomogenities in the sample may yield incorrect abundances of phases. Hillier (1999) has shown that most of these problems can be overcome by spray-drying the powdered sample using an air-brush and preparation of the spherical aggregates in conventional sample holders. In the present study, we attempted to reduce the preferred orientation of particles during sample preparation without this additional treatment and to correct the remaining influence of preferred orientation on the intensity distributions by the use of appropriate analytical models during the Rietveld refinement.

Initially, we tested two different ways of filling conventional top-loading holders with a powdered sample (WT22–163). In a first experiment, the powder was gently pressed into the top-loading holder, without a shearing motion, using the sharp edge of a sheet of glass. The surface was then carefully made rough with emery paper, and step-scan data were collected. The observed intensities of the strongest reflections in the XRD pattern were found to deviate significantly from the ideal ratios of intensities. Subsequently, the powder-filled top-loading holder was gold-coated and the surface of the powder was investigated with a Leica Stereoscan

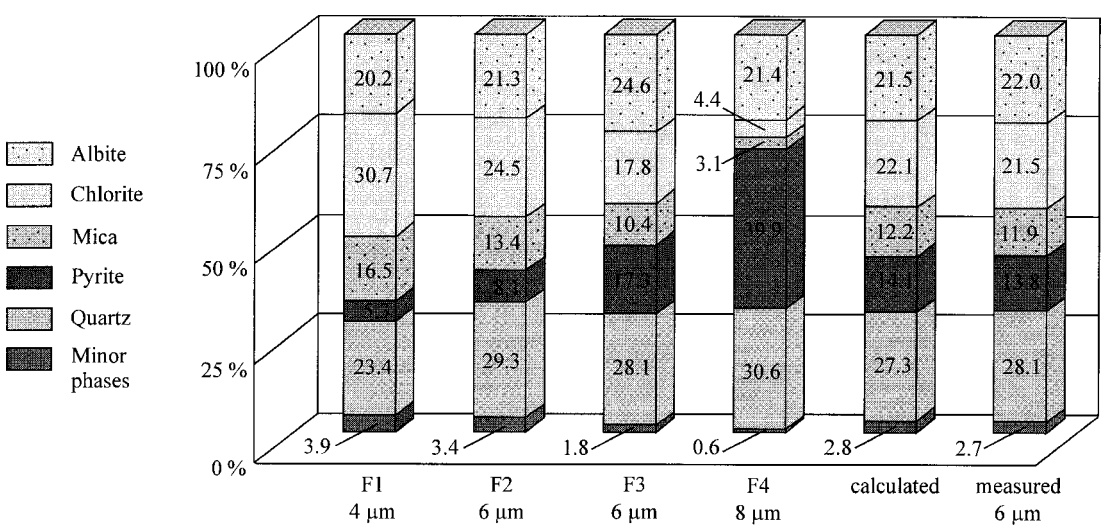

FIG. 1. Phase abundances (wt.%) and mean particle-sizes of four fractions (F1 to F4), the calculated, and the conventionally prepared sample WT22–163 (see text for explanation). Note that the mean particle-sizes are smaller in the phyllosilicate-rich fractions than in the samples containing substantial amounts of pyrite.

260 scanning electron microscope (SEM). The SEM was operated at 5 kV to allow inspection of the poorly conducting surface. A representative secondary electron (SE) image is shown in Figure 2. The figure illustrates that grain-size variations are remarkably large. The powder is densely loaded and large grains of plagioclase, quartz, and pyrite appear to be pressed into a loose matrix composed of phyllosilicate aggregates, yielding a relatively smooth surface. The orientations of the large grains appear to be controlled by the cleavage. Some of the phyllosilicate aggregates are smeared out and stick to the corners, edges, and surfaces of the larger grains.

In a second experiment, powder of the same sample was gently pressed into a holder with the sharp edge of a sheet of glass. Some additional powder was tapped through a sieve onto the holder. Because the grains have a more or less random orientation when falling from the sieve, a surface without strong preferred orientation of the particles was achieved. The sample obtained in this way was also investigated by XRD. Some significant deviations from the ideal intensity ratios of the strongest reflections of the constituent minerals were still observed, although the sample was less textured than in the first experiment. The surface of the powder was likewise studied under the SEM (Fig. 3). The powder in this top-loading holder appears to be more porous and exhibits more topography than that of the first experiment. Large grains of plagioclase, quartz, and pyrite are randomly distributed throughout a loose matrix dominated by the small aggregates of phyllosilicates. The differences in the observed deviations from the ideal intensity ratios as well as the results of the SEM study suggest that the effects of preferred orientation were minimized, at least to some extent, using the sample preparation applied in the second experiment. Therefore, the second method of preparation of the top-loading holders was routinely applied throughout the study.

The remaining effects of preferred orientation on the intensity distributions of the reflections in the diffraction patterns were corrected during Rietveld refinement. The algorithm used to model the *hkl*-dependency of the preferred orientation is described in detail by Bergmann *et al*. (2001). It is equivalent to models that expand the polar-axis density into a series of symmetrized spherical harmonics (Popa 1992, Järvinen 1993, Ferrari & Lutterotti 1994, Von Dreele 1997). The texture-correction yields *hkl*-specific correction factors of preferred orientation, which represent the ratio between the ideal intensity assuming a random orientation of the grains and the intensity taking preferred orientation into account. The suitability of the applied texture-model was tested for each phase by visualizing these correction factors for all possible crystallographic orientations of families of lattice planes, including those actually realized in the phase under investigation. The three-dimensional construction of all texture-correction factors of

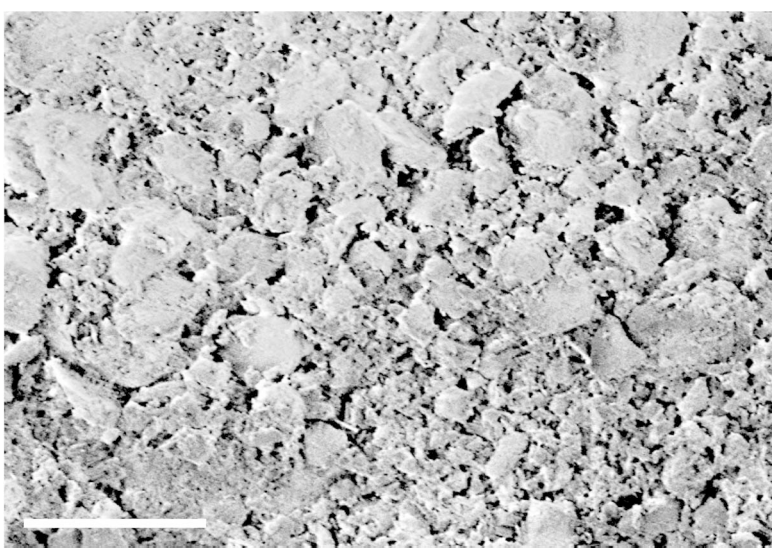

FIG. 2. Scanning electron microscope image of the strongly textured XRD powder sample WT22–163. The sample shows prominent grain-size variations although the powder was sieved using a 20 μm mesh. The surface of the powder was carefully roughed using emery paper. Preferred orientation of the grains in the powdered sample resulted in pronounced deviations from the ideal intensities in the XRD pattern. The scale bar is 25 μm.

FIG. 3. Scanning electron microscope image of a moderately textured XRD powder sample WT22–163. The large grain at the center is pyrite. The loose sample was obtained by tapping powder through a sieve on to the surface of the top-loading holder. The effects of preferred orientation of the grains on the intensity distribution in the XRD pattern was minimized by this method of sample preparation. The scale bar is 25 μm.

the phase under investigation is equivalent to the shape of the normalized polar-axis density and, therefore, gives a good visual impression whether the applied texture-model was physically reasonable. As an example, the shapes of the normalized polar-axis densities of epidote, muscovite, albite, and pyrite are shown in Figure 4. The shape of the polar-axis density of plagioclase can be accounted for by the perfect cleavages along {001} and {010}, whereas the preferred orientation of epidote was caused by the fairly good {001} cleavage. The shape of the polar-axis density of muscovite can be related to the very good {001} cleavage, whereas the preferred orientation of pyrite results from the shape of the crystals.

The texture description of all phases contained in the samples clearly introduces a large number of parameters to the Rietveld refinement. The information stored in the XRD patterns is usually insufficient to allow texture description of all phases using high orders of the texture models; resultant correlations among parameters may yield inaccurate results. Therefore, a scheme of parameter reduction was applied enabling routine analysis of the altered rocks characterized by pronounced differences in mineral abundances. The Rietveld refinement was started with different orders of the texture models for each phase contained in the multiphase sample because the extent of preferred orientation in a single top-loading holder is phase-specific. Therefore, a low order of the texture model was initially chosen for phases amenable to simple description of texture. Moreover, the order of the texture model was automatically reduced during Rietveld refinement as a function of the intensity of the phase after a first stage of isotropic refinement. The suitability of the texture model applied was checked routinely by inspection of the obtained list of peaks containing the *hkl*-specific correction factors of preferred orientation to ensure that no significant correlation of parameters occurred during the refinement. These correction factors should be in the range of 0.5 to 3 for slightly textured samples in conventional top-loading holders (Kleeberg & Bergmann 1998).

ROUTINE APPLICATION OF THE METHOD DEVELOPED

The proposed method of sample preparation and analysis was applied routinely to the 80 samples collected from the footwall of the Waterloo VHMS deposit. Sample preparation took approximately 30 min/sample, and data collection required a measurement time of 5.5 h/sample. Quantitative analysis of the multiphase samples was performed by refining approximately 140 independent parameters on the basis of 2,501 measured intensity values forming *ca.* 1,000 peaks in the diffraction patterns. The computation time required was approximately 5 to 10 minutes per diffraction pattern using the program AutoQuan running on a Pentium III 1,000 MHz personal computer. The refinement was conducted in fully automatic mode. The use of the program

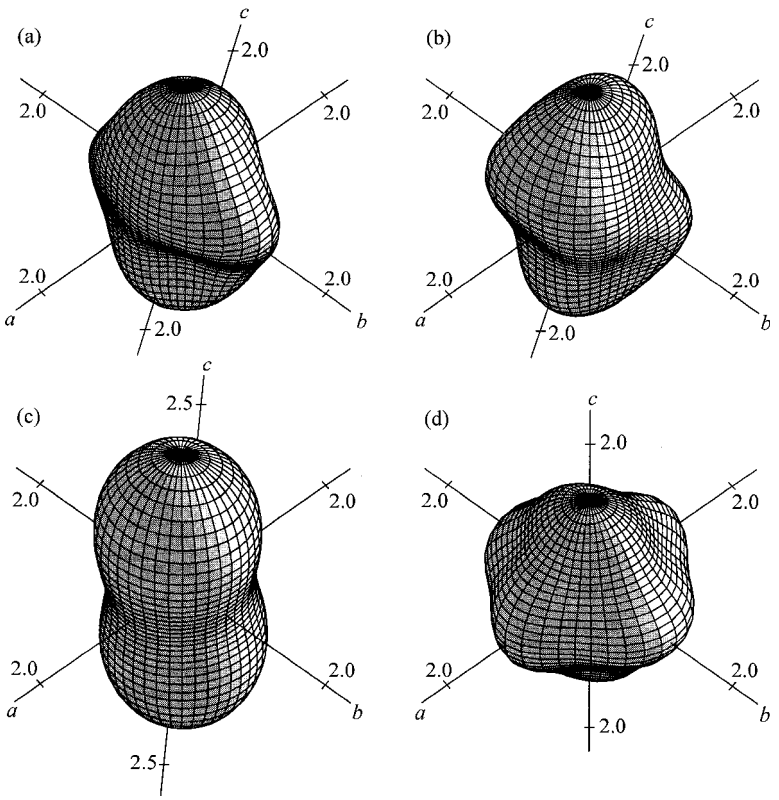

FIG. 4. Shapes of the normalized polar-axis densities of (a) albite, (b) epidote, (c) muscovite, and (d) pyrite (see text for explanation). The order of the texture model applied was n = 2 for muscovite, n = 4 for epidote and albite, and n = 6 for pyrite. The shapes of the polar-axis densities are primarily influenced by the orientation of the cleavage planes of the minerals.

AutoQuan proved to be particularly convenient because the measured and the calculated diffraction-patterns, as well as the difference curve, could be observed and compared with the peak positions of stored mineral structures during calculation. Therefore, the refinement was stopped as soon as peaks of an unidentified mineral phase appeared in the difference curve. This mineral phase was then identified by the search/match procedure and added to the list of constituent minerals. After careful qualitative analysis, this trial-and-error method rapidly led to the identification of all detectable mineral phases.

RESULTS AND DISCUSSION

The validity of the quantitative phase-analysis by the proposed method was evaluated in detail prior to geological interpretation of the results to constrain the precision and accuracy of the analytical results obtained on the samples from the Waterloo deposit.

Goodness of fit

The quality of the Rietveld refinement was assessed by inspection of the difference curve between the measured and the calculated XRD patterns and examination of numerical criteria of quality. A typical Rietveld refinement plot is given in Figure 5 to visualize the goodness of fit obtained between the measured and calculated intensities. The observed weighted residual errors R_{wp} ranged from approximately 6.5 to 14%, indicating very good agreement between the observed and simulated XRD patterns. Ideally, these weighted residual errors should approach the statistically expected values R_{exp} that ranged from 4 to 6%. The calculated goodness-of-fit values S ranged from approximately 1.5 to 2.5. In

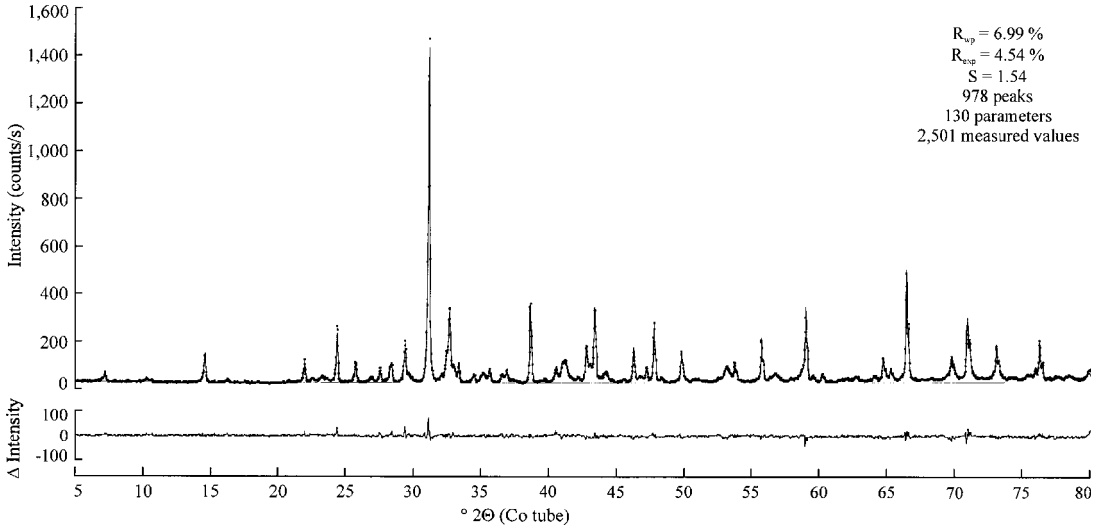

FIG. 5. Rietveld refinement plot of the sample WT22–163 (point: observed intensity at each step; solid line: calculated XRD pattern; thin line: fitted background; solid line below: difference curve between observed and calculated intensities).

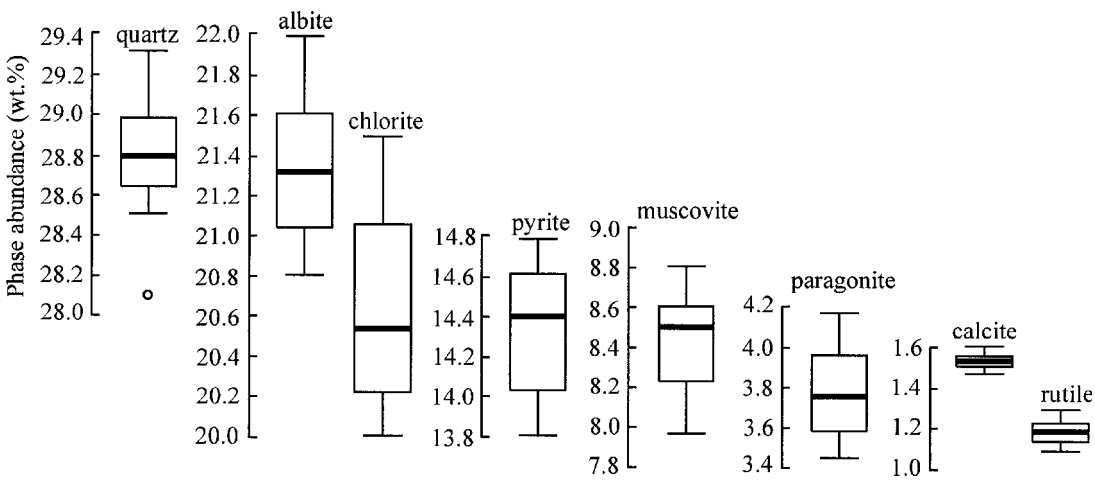

FIG. 6. Whisker-and-box plot representation of results of 10 independent preparations and analyses of the sample WT22–163. The box encloses the interquartile range with the median displayed as a line. The vertical lines extending outside the box mark the minimum and maximum values that fall within the acceptable range. The individual point is considered to be an outlier.

general, the observed S values were higher in the mica-rich samples than in samples containing low amounts of mica because layer disorder in the mica structures was not considered in the present study.

Precision

To evaluate the precision of the proposed method, the sample preparation of the powder WT22–163 (sieving and grinding of the powder obtained from disc milling, homogenization, and preparation of top-loading sample holders) and the XRD data collection was repeated ten times under standard conditions. The ten XRD patterns were refined in fully automatic mode using identical starting parameters and model settings. A whisker-and-box plot of the results obtained is given in Figure 6. The interquartile range of the major rock-forming minerals was observed to be in the range of 0.5

wt.%. The acceptable range for major phases is in the order of 1 to 1.5 wt.%. The closeness of the replicate determinations shows that random within-laboratory errors were relatively small. The observed spread in the data can be primarily accounted for by loss of sample powder during the process of sieving and grinding (*e.g.*, dust production) and the preparation of the top-loading sample holders (*e.g.*, different degrees of preferred orientation).

Accuracy

The accuracy of the quantitative XRD analysis is difficult to demonstrate for the samples investigated because appropriate reference-materials are not available and the composition of the altered rocks is highly variable. Although synthetic rocks could be prepared as weighed mixtures of pure minerals, such in-house reference materials would undoubtedly have different physical properties (*e.g.*, strain and crystallite sizes) and chemical compositions (*e.g.*, cation occupancies), hampering their direct applicability. However, the quantitative phase-analysis by the Rietveld method can be evaluated by expressing the modal abundance of minerals in the rocks as chemical compositions and comparing them to the whole-rock XRF data.

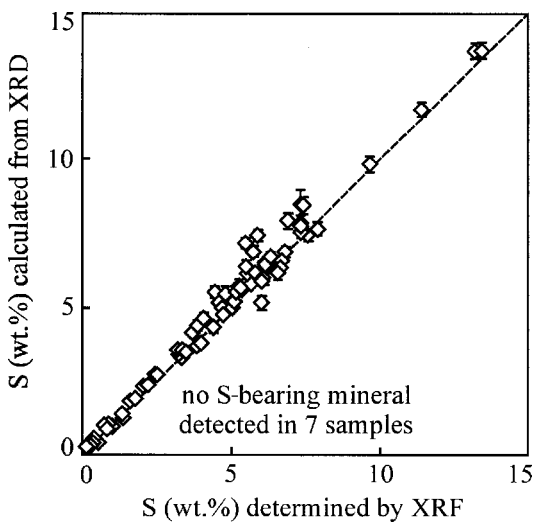

FIG. 7. Plot of the sulfur contents of the hydrothermally altered rocks obtained by recalculation of the XRD results *versus* XRF data. The error bars are based on 3σ errors of the sulfur-bearing phases as determined by the Rietveld refinement. Errors of the XRF are smaller than the symbol size. The plot indicates that the effects of micro-absorption were successfully minimized during routine application of the method developed.

The recalculation of XRD results was performed by assuming ideal compositions of minerals except where the cation occupancies were refined as a part of the Rietveld analysis. Routine recalculation of the phase compositions and comparison with the geochemical results proved to be a useful test of systematic errors in the quantitative XRD analysis. Figure 7 shows a comparison of the sulfur concentrations derived from the recalculation of the sulfide contents of the samples and the sulfur concentrations determined by XRF. Because no systematic difference was observed, we conclude that the effects of micro-absorption were successfully minimized. Similar plots are given in Figure 8 for other major elements. The recalculated SiO_2 content of many samples seem to be only slightly overestimated, whereas the Al_2O_3 contents were commonly underestimated in comparison to the XRF results. A similar relationship was observed for the recalculated MgO and Fe_2O_3 concentrations. Figure 8 also shows that the agreement between the recalculated Na_2O and K_2O and the directly measured values is excellent, taking into account that peak overlap between the various species of dioctahedral mica is pronounced and may lead to significant correlation among parameters during refinement. From Figure 8, it is clear that the phase abundance and refined occupancies of cations were accurately determined by the Rietveld method. The observed slight deviations can be accounted for by the non-ideal compositions of the constituent minerals and possible substitutions among cations in the alteration minerals that were not considered in the Rietveld refinement. However, the presence of minor phases (below detection limits of the XRD) as well as refinement errors may also yield some differences between the recalculated XRD results and the XRF data.

Phase abundance

The altered rocks investigated from the Waterloo deposit contain up to 10 detectable phases. Hierarchical cluster analysis performed on the basis of the quantitative abundances of phases showed that the samples can

FIG. 8. Plots of major-element concentrations of the hydrothermally altered rocks obtained by recalculation of the XRD results *versus* XRF data (both datasets are renormalized to 100% anhydrous). The error bars are based on 3σ errors of concentrations of the rock-forming minerals as determined by the Rietveld refinement. Errors associated with the XRF data are smaller than the symbol size. The plots demonstrate that the phase abundances and refined occupancies of cations were accurately determined during routine application of the method developed.

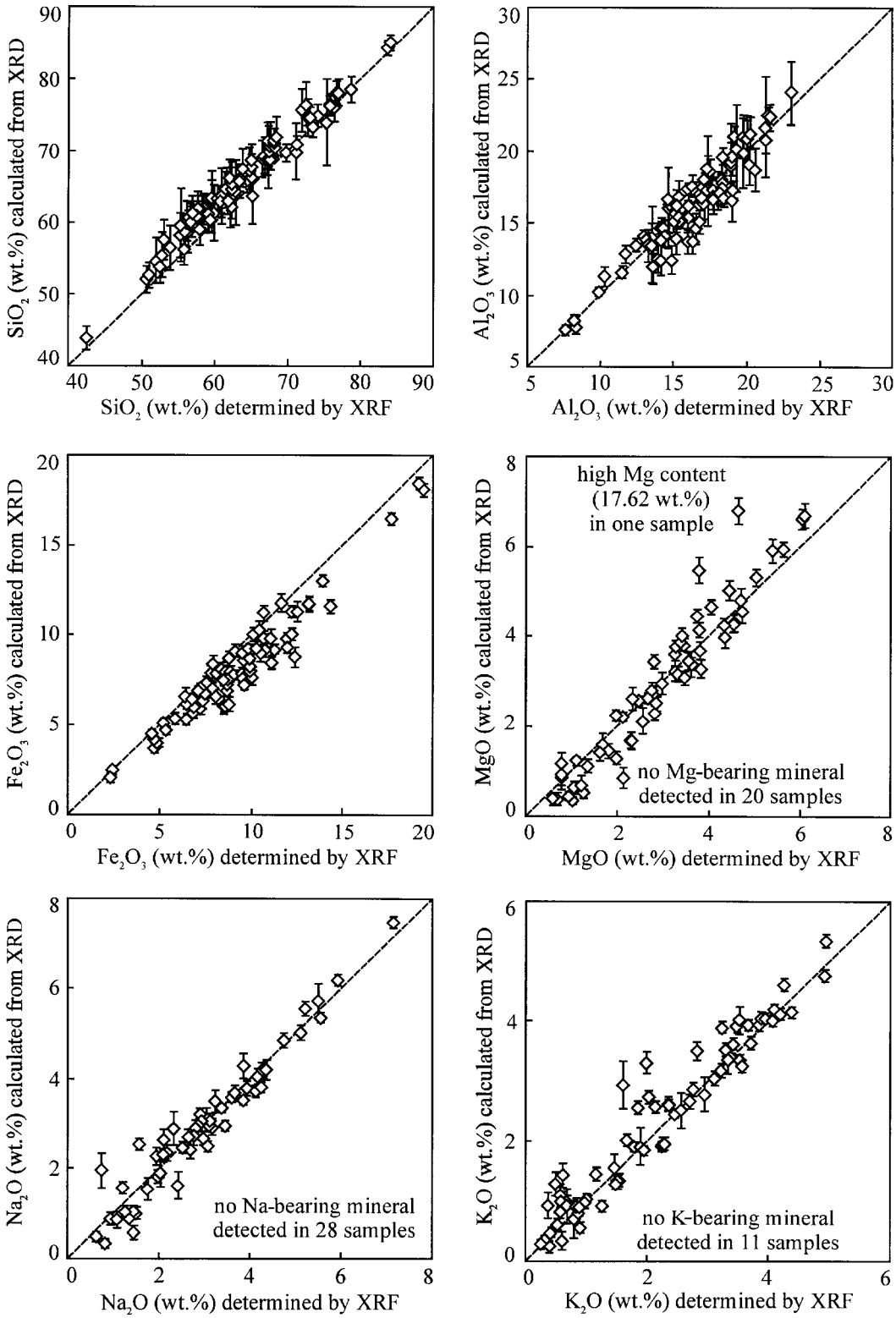
SiO2 (wt.%) calculated from XRD
SiO2 (wt.%) determined by XRF
Al2O3 (wt.%) calculated from XRD
Al2O3 (wt.%) determined by XRF
Fe2O3 (wt.%) calculated from XRD
Fe2O3 (wt.%) determined by XRF
MgO (wt.%) calculated from XRD
high Mg content
(17.62 wt.%)
in one sample
no Mg-bearing mineral
detected in 20 samples
MgO (wt.%) determined by XRF
Na2O (wt.%) calculated from XRD
no Na-bearing mineral
detected in 28 samples
Na2O (wt.%) determined by XRF
K2O (wt.%) calculated from XRD
no K-bearing mineral
detected in 11 samples
K2O (wt.%) determined by XRF

be grouped into seven distinct alteration-induced assemblages (Fig. 9). The mineralogical compositions of representative samples from these assemblages are given in Tables 2 to 4, together with their respective estimated random errors (3σ). These errors were derived from the uncertainties in the Rietveld scale-factors and are typically ≤0.5 wt.% for minor phases and range from 0.5 to 1.5 wt.% for major rock-forming minerals.

The alteration-induced assemblages distinguished are characteristic of specific zones of alteration, which show a strong spatial zonality with respect to the mineralization (Fig. 10). The innermost zone underlying the massive sulfide lenses is silicic and consists of an alteration-induced assemblage of pyrite, quartz, muscovite with minor amounts of rutile (Table 2). The quartz content varies from approximately 45 to 75 wt.%. In all samples investigated, the muscovite content was found to be lower than that of quartz. Samples from this assemblage contain up to 25 wt.% pyrite. Chlorite and calcite are not present. The zone of silicic alteration is locally enveloped by a zone of phyllic–argillic alteration (Table 2). This zone of alteration is typified by an as-

TABLE 2. RESULTS OF THE RIETVELD REFINEMENT OF SELECTED SAMPLES FROM THE SILICIC AND PHYLLIC-ARGILLIC ALTERATION ZONES OF THE FOOTWALL ALTERATION HALO OF THE WATERLOO VHMS DEPOSIT

	Pyrite – quartz – muscovite assemblage			Pyrite – muscovite – pyrophyllite kaolinite – Na–K mica paragonite – quartz assemblage		
	WT2-421	WT2-440	WT16-276	WT7-171	WT16-245	WT16-257
Kaolinite	-	-	-	1.0 ± 0.6	4.7 ± 0.9	3.0 ± 0.8
Muscovite	19.2 ± 1.1	18.3 ± 1.3	36.2 ± 1.0	15.4 ± 2.4	16.7 ± 3.9	38.2 ± 2.0
Na–K mica	-	-	-	8.2 ± 2.1	8.3 ± 1.2	8.8 ± 1.3
Paragonite	-	-	-	4.4 ± 1.1	-	4.1 ± 0.8
Pyrite	25.1 ± 0.5	24.7 ± 0.5	6.0 ± 0.3	18.1 ± 0.5	9.0 ± 0.6	7.2 ± 0.4
Pyrophyllite	-	-	-	3.6 ± 0.8	11.7 ± 1.6	5.1 ± 1.0
Quartz	55.3 ± 0.8	56.6 ± 1.0	56.8 ± 1.0	47.8 ± 1.0	48.3 ± 2.2	31.4 ± 1.0
Rutile	0.4 ± 0.2	0.4 ± 0.2	1.0 ± 0.3	1.5 ± 0.4	1.3 ± 0.5	2.2 ± 0.5
R_{wp} %	8.66	8.71	11.72	7.58	11.70	11.36
R_{exp} %	5.18	5.49	5.53	5.29	4.93	4.71
S	1.67	1.59	2.12	1.43	2.37	2.41

Notes: R_{wp}: weighted resitual error, R_{exp}: expected error, S: goodness of fit. Proportion of phases in wt.%.

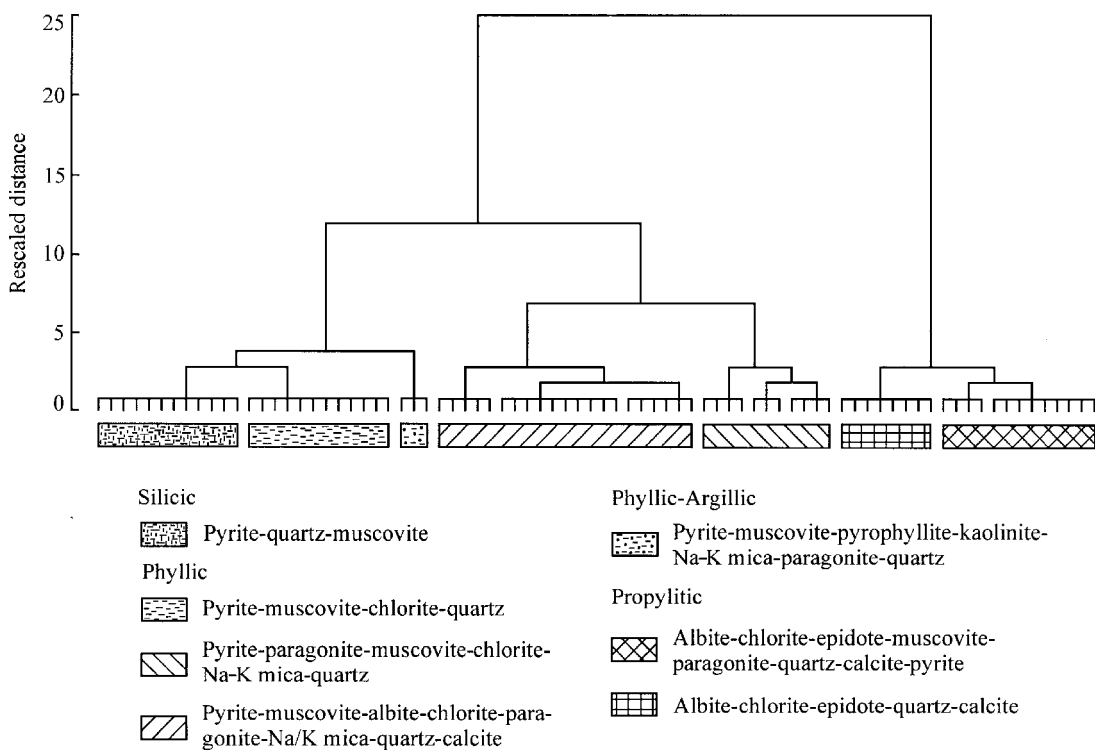

FIG. 9. Dendrogram resulting from hierarchical cluster analysis of the quantitative phase-abundances (Ward's method performed on centered-log-ratio-transformed data). The dendrogram shows that seven mineralogically distinct alteration-induced assemblages can be identified in the footwall alteration-induced halo of the Waterloo VHMS deposit.

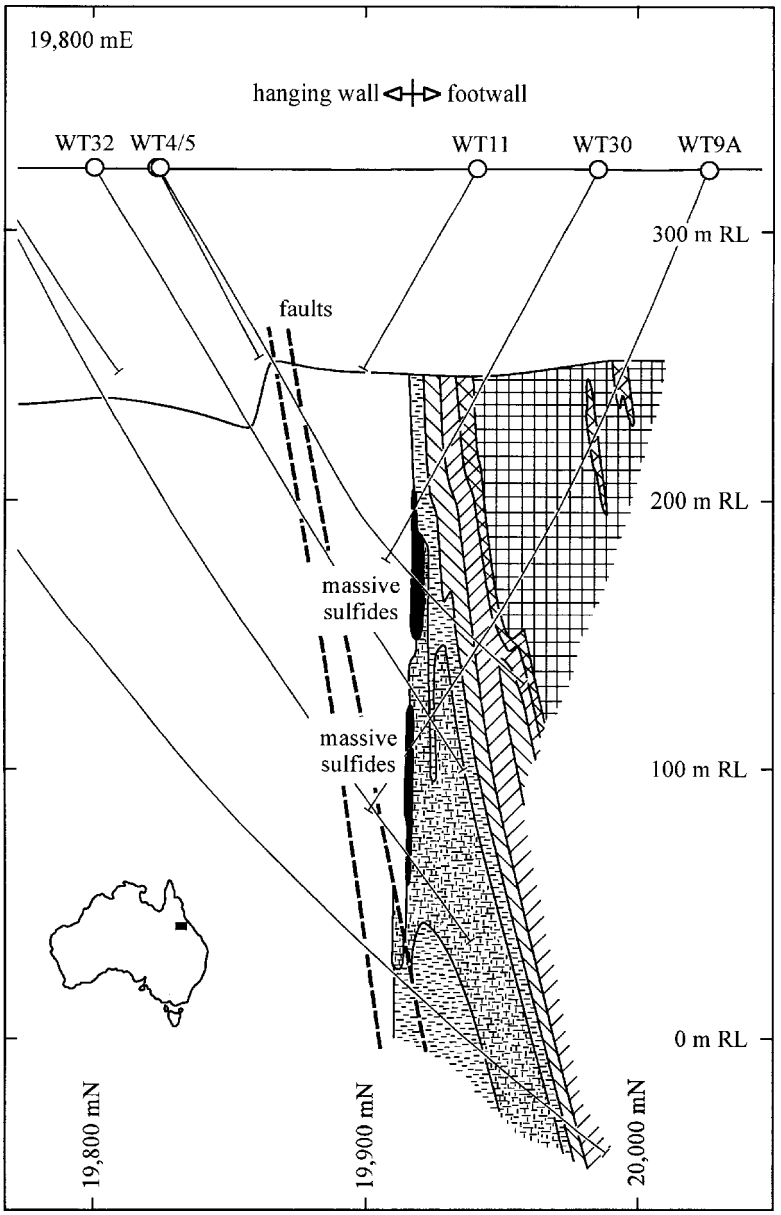

FIG. 10. Cross-section of the Waterloo VHMS deposit showing the spatial distribution of the alteration assemblages in the footwall alteration halo. Note that the massive sulfides and the volcanic wallrocks were turned into a subvertical position during regional deformation. Map patterns as in Figure 9.

semblage of pyrite, muscovite, pyrophyllite, kaolinite, Na–K mica, paragonite, quartz, and minor rutile. The quartz content of the samples from this assemblage is usually lower than that in the rocks collected from the zone of silicic alteration. Muscovite is the most abundant phyllosilicate in the samples from the phyllic–argillic alteration zone. The contents of pyrophyllite and kaolinite range up to 5 and 15 wt.%, respectively. The

TABLE 3. RESULTS OF THE RIETVELD REFINEMENT OF SELECTED SAMPLES FROM THE PHYLLIC ALTERATION ZONES OF THE FOOTWALL ALTERATION HALO OF THE WATERLOO VHMS DEPOSIT

	Pyrite – muscovite – chlorite quartz assemblage			Pyrite – paragonite – muscovite chlorite – Na–K mica – quartz assemblage			Pyrite – muscovite – albite chlorite – paragonite Na–K-mica – quartz – calcite assemblage		
	WT22-244	WT22-256	WT22-264	WT16-125	WT16-170	WT22-208	WT22-148	WT22-163	WT22-222
Albite	-	-	-	-	-	-	38.4 ± 1.1	22.0 ± 1.3	5.8 ± 0.8
Calcite	-	-	-	1.5 ± 0.3	-	-	1.3 ± 0.3	1.6 ± 0.3	1.6 ± 0.3
Chlorite	1.8 ± 0.7	6.1 ± 0.9	2.2 ± 0.5	4.8 ± 0.7	2.2 ± 0.8	14.6 ± 0.9	2.5 ± 0.6	21.5 ± 0.9	11.8 ± 0.8
Muscovite	33.3 ± 0.8	46.4 ± 1.1	38.3 ± 0.9	23.9 ± 2.0	19.4 ± 2.1	13.8 ± 0.9	12.7 ± 1.3	8.2 ± 0.9	25.9 ± 1.3
Na–K mica	-	-	-	7.7 ± 2.3	11.3 ± 2.2	-	5.3 ± 2.2	-	-
Paragonite	-	-	-	12.5 ± 1.6	14.3 ± 2.5	10.0 ± 0.8	6.1 ± 1.6	3.7 ± 0.7	3.0 ± 0.6
Pyrite	11.0 ± 0.3	12.5 ± 0.4	11.9 ± 0.3	11.6 ± 0.5	14.0 ± 0.5	11.5 ± 0.5	14.8 ± 0.4	13.8 ± 0.5	7.7 ± 0.3
Quartz	53.2 ± 0.8	35.0 ± 0.9	47.1 ± 0.7	37.1 ± 1.0	37.4 ± 1.0	48.6 ± 1.0	18.7 ± 0.6	28.1 ± 0.8	43.6 ± 1.0
Rutile	0.7 ± 0.2	-	0.5 ± 0.2	0.9 ± 0.3	1.4 ± 0.3	1.5 ± 0.3	0.2 ± 0.1	1.1 ± 0.4	0.6 ± 0.2
R_{wp} %	7.51	10.20	8.01	9.13	9.66	10.92	6.96	8.86	8.66
R_{exp} %	4.64	5.13	4.54	4.82	4.67	5.06	4.16	4.75	5.89
S	1.62	1.99	1.76	1.89	2.07	2.16	1.67	1.87	1.47

Notes: R_{wp}: weighted resitual error, R_{exp}: expected error, S: goodness of fit. Proportion of phases in wt.%.

TABLE 4. RESULTS OF THE RIETVELD REFINEMENT OF SELECTED SAMPLES FROM THE PROPYLITIC ALTERATION ZONE OF THE FOOTWALL ALTERATION HALO OF THE WATERLOO VHMS DEPOSIT

	Albite – chlorite – epidote muscovite – paragonite – quartz calcite – pyrite assemblage			Albite – chlorite – epidote quartz – calcite assemblage		
	WT16-145	WT16-186	WT22-100	WT9A-126	WT9A-144	WT16-132
Albite	30.7 ± 1.0	20.8 ± 1.0	19.8 ± 1.1	29.3 ± 0.9	23.9 ± 0.9	50.3 ± 1.1
Calcite	4.1 ± 0.4	5.1 ± 0.4	4.6 ± 0.4	3.2 ± 0.3	3.9 ± 0.4	3.5 ± 0.5
Chlorite	21.3 ± 0.8	20.4 ± 0.8	14.4 ± 0.8	23.3 ± 0.9	16.5 ± 0.9	21.7 ± 0.9
Epidote	4.5 ± 0.6	14.0 ± 0.7	16.5 ± 0.8	16.2 ± 0.7	37.8 ± 0.8	7.0 ± 0.8
Muscovite	4.0 ± 0.7	5.6 ± 0.7	-	-	-	-
Paragonite	4.5 ± 0.6	5.7 ± 0.6	5.0 ± 0.7	-	-	-
Pyrite	3.9 ± 0.2	-	2.6 ± 0.2	-	-	2.5 ± 0.2
Quartz	27.0 ± 0.7	27.7 ± 0.7	37.1 ± 0.9	24.6 ± 0.5	14.4 ± 0.4	15.0 ± 0.6
Rutile	-	0.7 ± 0.2	-	-	-	-
Titanite	-	-	-	3.4 ± 0.5	3.5 ± 0.5	-
R_{wp} %	7.50	6.87	7.54	6.42	6.47	7.80
R_{exp} %	3.95	4.06	4.22	4.05	4.18	4.05
S	1.90	1.69	1.79	1.59	1.55	1.93

Notes: R_{wp}: weighted resitual error, R_{exp}: expected error, S: goodness of fit. Proportion of phases in wt.%.

concentration of pyrite varies from 5 to 20 wt.%. Chlorite and calcite also are absent from the zone of phyllic–argillic alteration.

The zone of silicic alteration typically grades outward into a zone of phyllic alteration. The XRD study revealed that this zone consists of three distinct alteration-induced assemblages (Table 3). The alteration-induced assemblage in the inner part of the zone of phyllic alteration proximal to the massive sulfides is characterized by pyrite, muscovite, chlorite, quartz, and rutile. Muscovite and quartz are the most abundant minerals in this alteration-induced assemblage. The chlorite contents are variable and range from approximately 2 to 15 wt.%. With increasing distance to the massive sulfides, this alteration-induced assemblage grades into an assemblage consisting of pyrite, paragonite, muscovite, chlorite, Na–K mica, quartz, as well as minor calcite and rutile. The dioctahedral mica, quartz, and chlorite represent the most important rock-forming minerals. Calcite is present in some samples only from this alteration-induced assemblage. The peripheral parts of the zone of phyllic alteration are typified by the mineral assemblage pyrite, muscovite, albite, chlorite, paragonite, Na–K mica, quartz, calcite, and minor rutile. Muscovite, albite, paragonite, quartz, and chlorite are the major components of samples from this alteration-induced assemblage. The concentration of albite varies between 5 and 40 wt.%.

The fringes of the footwall alteration halo are characterized by a zone of propylitic alteration (Table 4). This zone consists of two mineralogically distinct assemblages. The mineral assemblage reflecting more intense hydrothermal alteration is typified by albite, chlorite, epidote, muscovite, paragonite, quartz, calcite, pyrite, and minor rutile. The chlorite and epidote contents in samples from this mineral assemblage range from 5 to 30 and 1 to 25 wt.%, respectively. The other assemblage of minerals in the zone of propylitic alter-

ation lacks dioctahedral mica. This assemblage is characterized by albite, chlorite, epidote, quartz, calcite, and minor amounts of titanite. Samples from this alteration-induced assemblage are typified by substantial amounts of chlorite and epidote. The pyrite content is typically very low (<3 wt.%).

The XRD results presented above reveal that the mineralogy of the footwall alteration halo is relatively complex, primarily reflecting variations in the extent of hydrolytic decomposition of the andesitic host-rocks. The types of resulting alteration-induced assemblages range from intense hydrolytic alteration, represented by the silicic and the phyllic–argillic alteration, to weak and incipient hydrolytic alteration represented by the propylitic assemblages (Fig. 10). In addition, potassium metasomatism appears to have played a major role in the formation of the observed assemblages of minerals.

Conclusions

In the present study, a scheme of sample preparation, measurement and analysis was developed that allows a reliable quantification of the phase abundances in hydrothermally altered rocks. Experiments were carried out to reduce systematic errors associated with the method. We found that the effects of micro-absorption can be sufficiently minimized by fine grinding of the samples (<20 μm), the use of Co$K\alpha$ radiation, and particle-size correction during Rietveld refinement. Different techniques of sample preparation were tested to reduce the extent of preferred orientation of the particles. The choice of appropriate models of the texture during Rietveld refinement allows a correct description of the remaining effects of preferred orientation.

The proposed method of sample preparation and analysis was evaluated using samples from the altered zone in the footwall of the Waterloo VHMS deposit, Australia. The samples investigated are characterized by highly variable mineralogical compositions and contain up to 10 phases, causing substantial overlap of peaks in XRD patterns. We demonstrate that with the Rietveld program BGMN/AutoQuan, we were able to refine these complex diffraction patterns in fully automatic mode without user-defined refinement strategy. The results obtained were shown to be precise and accurate. The results of the quantitative phase-analysis were used to discriminate mineralogically distinct alteration-induced assemblages. We found that these assemblages are characteristic of several alteration zones that occur spatially disposed with respect to the massive sulfides. Thus, the routine phase-analysis of altered rocks by the methods proposed will enable economic geologists to quantify alteration-induced assemblages and to distinguish alteration zones associated with VHMS-type deposits.

Acknowledgements

We express our gratitude to J. Bergmann for the development of the versatile Rietveld software and discussion of the experimental results. We are especially grateful to J.E. Post, R.F. Martin, and an anonymous reviewer, who helped us improve an earlier version of the manuscript. J. Monecke is thanked for valuable comments and remarks improving the applicability of the texture model. We are also indebted to W. Zahn for taking the SEM pictures and to P. Robinson for carrying out the major-element analyses. We gratefully acknowledge analytical support by N. Hlaing and K. McGoldrick. G. Werner kindly provided access to the laser-based particle-size-distribution granulometer. TM thanks the Studienstiftung des Deutschen Volkes for financial support. PMH acknowledges support by the Leibniz Program of the Deutsche Forschungsgemeinschaft. The Deutsche Forschungsgemeinschaft (KL 1286/1–1 and KL 1286/1–2), the Australian Research Council's Research Centres Program, the AMIRA P439 project, and RGC Exploration Ltd. supported the research.

References

Barrett, T.J., Cattalani, S. & MacLean, W.H. (1993): Volcanic lithogeochemistry and alteration at the Delbridge massive sulfide deposit, Noranda, Quebec. *J. Geochem. Explor.* **48**, 135-173.

Bergmann, J., Friedel, P. & Kleeberg, R. (1998): BGMN – a new fundamental parameters based Rietveld program for laboratory X-ray sources, its use in quantitative analysis and structure investigations. *CPD Newslett.* **20**, 5-8.

_____ & Kleeberg, R. (1998): Rietveld analysis of disordered layer silicates. *In* EPDIC 5 – Proc. European Powder Diffraction Conf. (R. Delhez & E.J. Mittemeijer, eds.). *Mat. Sci. Forum* **278-281**, 300-305.

_____, _____ , Haase, A. & Breidenstein, B. (2000): Advanced fundamental parameter model for improved profile analysis. *In* EPDIC 6 – Proc. European Powder Diffraction Conf. (R. Delhez & E.J. Mittemeijer, eds.). *Mat. Sci. Forum* **347-349**, 303-308.

_____ , _____ & Taut, T. (1994): A new structure refinement and quantitative phase analysis method basing on predetermined true peak profiles. *Z. Kristallogr., Suppl.* **8**, 580.

_____ , _____ & _____ (1997): Quantitative phase analysis using a new Rietveld algorithm – assisted by improved stability and convergence behavior. *Adv. X-Ray Anal.* **40**, 425.

_____ , Monecke, T. & Kleeberg, R. (2001): Alternative algorithm for the correction of preferred orientation in Rietveld analysis. *J. Appl. Crystallogr.* **34**, 16-19.

BERRY, R.F., HUSTON, D.L., STOLZ, A.J., HILL, A.P., BEAMS, S.D., KURONEN, U. & TAUBE, A. (1992): Stratigraphy, structure, and volcanic-hosted mineralization of the Mount Windsor Subprovince, North Queensland, Australia. *Econ. Geol.* **87**, 739-763.

BISH, D.L. (1993): Studies of clays and clay minerals using X-ray powder diffraction and the Rietveld method. *In* CMS Workshop Lectures. 5. Computer Applications to X-ray Powder Diffraction Analysis of Clay Minerals (R.C. Reynolds, Jr. & J.R. Walker, eds.). The Clay Minerals Society, Boulder, Colorado (79-121).

_____ & HOWARD, S.A. (1988): Quantitative phase analysis using the Rietveld method. *J. Appl. Crystallogr.* **21**, 86-91.

_____ & POST, J.E. (1993): Quantitative mineralogical analysis using the Rietveld full-pattern method. *Am. Mineral.* **78**, 932-940.

_____ & REYNOLDS, R.C., JR. (1989): Sample preparation for X-ray diffraction. *In* Modern Powder Diffraction (D.L. Bish & J.E. Post, eds.). *Rev. Mineral.* **20**, 73-99.

_____ & VON DREELE, R.B. (1989): Rietveld refinement of non-hydrogen atomic positions in kaolinite. *Clays Clay Minerals* **37**, 289-296.

BRINDLEY, G.W. (1945): The effect of grain or particle size on X-ray reflections from mixed powders and alloys, considered in relation to the quantitative determination of crystalline substances by X-ray methods. *Philos. Mag.* **36**, 347-369.

BROSTIGEN, G. & KJEKSHUS, A. (1969): Redetermined crystal structure of FeS_2 (pyrite). *Acta Chem. Scand.* **23**, 2186-2188.

COMODI, P. & ZANAZZI, P.F. (1995): High-pressure structural study of muscovite. *Phys. Chem. Minerals* **22**, 170-177.

DOLLASE, W.A. (1971): Refinement of the crystal structures of epidote, allanite and hancockite. *Am. Mineral.* **56**, 447-464.

EFFENBERGER, H., MEREITER, K. & ZEMANN, J. (1981): Crystal structure refinements of magnesite, calcite, rhodochrosite, siderite, smithonite, and dolomite, with discussion of some aspects of the stereochemistry of calcite type carbonates. *Z. Kristallogr.* **156**, 233-243.

FERRARI, M. & LUTTEROTTI, L. (1994): Method for the simultaneous determination of anisotropic residual stresses and texture by X-ray diffraction. *J. Appl. Phys.* **76**, 7246-7255.

FRANKLIN, J.M., LYDON, J.W. & SANGSTER, D.F. (1981): Volcanic-associated massive sulfide deposits. Econ. Geol., 75th Anniv. Vol., 485-627.

GEMMELL, J.B. & LARGE, R.R. (1992): Stringer system and alteration zones underlying the Hellyer volcanic-hosted massive sulfide deposit, Tasmania, Australia. *Econ. Geol.* **87**, 620-649.

GUALTIERI, A.F. (2000): Accuracy of XRPD QPA using the combined Rietveld–RIR method. *J. Appl. Crystallogr.* **33**, 267-278.

GUIRADO, F., GALI, S. & CHINCHÓN, S. (2000): Quantitative Rietveld analysis of aluminous cement clinker phases. *Cem. Concr. Res.* **30**, 1023-1029.

GÜVEN, N. (1971): The crystal structures of $2M_1$ phengite and $2M_1$ muscovite. *Z. Kristallogr.* **134**, 196-212.

HENDERSON, R.A. (1986): Geology of the Mt Windsor Subprovince – a lower Palaeozoic volcano-sedimentary terrane in the northern Tasman Orogenic Zone. *Aust. J. Earth Sci.* **33**, 343-364.

HILL, R.J. & HOWARD, C.J. (1987): Quantitative phase analysis from neutron powder diffraction data using the Rietveld method. *J. Appl. Crystallogr.* **20**, 467-474.

_____ , TSAMBOURAKIS, G. & MADSEN, I.C. (1993): Improved petrological modal analyses from X-ray powder diffraction data by use of the Rietveld method. I. Selected igneous, volcanic, and metamorphic rocks. *J. Petrol.* **34**, 867-900.

HILLIER, S. (1999): Use of an air brush to spray dry samples for X-ray powder diffraction. *Clay Minerals* **34**, 127-135.

_____ (2000): Accurate quantitative analysis of clay and other minerals in sandstone by XRD: comparison of a Rietveld and a reference intensity ratio (RIR) method and the importance of sample preparation. *Clay Minerals* **35**, 291-302.

HÖLZER, G., FRITSCH, M., DEUTSCH, M., HÄRTWIG, J. & FÖRSTER, E. (1997): $K\alpha_{1,2}$ and $K\beta_{1,3}$ X-ray emission lines of the 3*d* transition metals. *Phys. Rev.* **A56**, 4554-4568.

HUSTON, D.L., KURONEN, U. & STOLZ, J. (1995): Waterloo and Agincourt prospects, northern Queensland: contrasting styles of mineralization within the same volcanogenic hydrothermal system. *Aust. J. Earth Sci.* **42**, 203-221.

JÄRVINEN, M. (1993): Application of symmetrized harmonics expansion to correction of the preferred orientation effect. *J. Appl. Crystallogr.* **26**, 525-531.

KLEEBERG, R. & BERGMANN, J. (1998): Quantitative Röntgenphasenanalyse mit den Rietveld-Programmen BGMN und AUTOQUANT in der täglichen Laborpraxis. *Ber. DTTG* **6**, 237-250.

LARGE, R.R. (1992): Australian volcanic-hosted massive sulfide deposits: features, styles, and genetic models. *Econ. Geol.* **87**, 471-510.

LEISTEL, J.M., MARCOUX, E., THIÉBLEMONT, D., QUESADA, C., SÁNCHEZ, A., ALMODÓVAR, G.R., PASCUAL, E. & SÁEZ, R. (1998): The volcanic-hosted massive sulphide deposits of the Iberian Pyrite Belt: review and preface to the thematic issue. *Mineral. Deposita* **33**, 2-30.

MADSEN, I.C., SCARLETT, N.V.Y., CRANSWICK, L.M.D. & LWIN, T. (2001): Outcomes of the International Union of Crystallography Commission on Powder Diffraction round robin on quantitative phase analysis: samples 1a to 1h. *J. Appl. Crystallogr.* **34**, 409-426.

MARQUIS, P., BROWN, A.C., HUBERT, C. & RIGG, D.M. (1990): Progressive alteration associated with auriferous massive sulfide bodies at the Dumagami mine, Abitibi greenstone belt, Quebec. *Econ. Geol.* **85**, 746-764.

MEAGHER, E.P. & LAGER, G.A. (1979): Polyhedral thermal expansion in the TiO_2 polymorphs. Refinement of the crystal structures of rutile and brookite at high temperature. *Can. Mineral.* **17**, 77-85.

MONECKE, T., HERZIG, P.M., KLEEBERG, R., KÖHLER, S. & GEMMELL, J.B. (2000): Zonation of dioctahedral true mica species in the footwall alteration halo of the Waterloo VHMS deposit, northern Queensland, Australia. *In* Volcanic Environments and Massive Sulfide Deposits (J.B. Gemmell & J. Pongratz, eds.). CODES SRC, Hobart, Australia (131-133).

MUMME, W.G., TSAMBOURAKIS, G., MADSEN, I.C. & HILL, R.J. (1996): Improved petrological modal analyses from X-ray powder diffraction data by use of the Rietveld method. II. Selected sedimentary rocks. *J. Sed. Res.* **66**, 132-138.

POPA, N.C. (1992): Texture in Rietveld refinement. *J. Appl. Crystallogr.* **25**, 611-616.

RAUDSEPP, M., PANI, E. & DIPPLE, G.M. (1999): Measuring mineral abundance in skarn. I. The Rietveld method using X-ray powder-diffraction data. *Can. Mineral.* **37**, 1-15.

RICHARDS, H.G., CANN, J.R. & JENSENIUS, J. (1989): Mineralogical zonation and metasomatism of the alteration pipes of Cyprus sulfide deposits. *Econ. Geol.* **84**, 91-115.

RIETVELD, H.M. (1969): A profile refinement method for nuclear and magnetic structures. *J. Appl. Crystallogr.* **2**, 65-71.

RULE, A.C. & BAILEY, S.W. (1987): Refinement of the crystal structure of a monoclinic ferroan clinochlore. *Clays Clay Minerals* **35**, 129-138.

SIDORENKO, O.V., ZVYAGIN, B.B. & SOBOLEVA, S.V. (1977): Refinement of the crystal structure of $2M_1$ paragonite by the method of high-voltage electron diffraction. *Sov. Phys. Crystallogr.* **22**, 554-556.

SNYDER, R.L. & BISH, D.L. (1989): Quantitative analysis. *In* Modern Powder Diffraction (D.L. Bish & J.E. Post, eds.). *Rev. Mineral.* **20**, 101-144.

STOLZ, A.J. (1995): Geochemistry of the Mount Windsor Volcanics: implications for the tectonic setting of Cambro-Ordovician volcanic-hosted massive sulfide mineralization in northeastern Australia. *Econ. Geol.* **90**, 1080-1097.

TAUT, T., KLEEBERG, R. & BERGMANN, J. (1997): The new Seifert Rietveld program and its application to quantitative phase analysis. *In* Proc. XVII Conf. on Applied Crystallography (H. Morawiec & D. Stróz, eds.). World Scientific, Singapore (87-92).

TAYLOR, J.C. & MATULIS, C.E. (1991): Absorption contrast effects in the quantitative XRD analysis of powders by full multi-phase profile refinement. *J. Appl. Crystallogr.* **24**, 14-17.

TAYLOR, M. & BROWN, G.E. (1976): High-temperature structural study of the $P2_1/a \leftrightarrow A2/a$ phase transition in synthetic titanite, $CaTiSiO_5$. *Am. Mineral.* **61**, 435-447.

URABE, T. & SCOTT, S.D. (1983): Geology and footwall alteration of the South Bay massive sulphide deposit, northwestern Ontario, Canada. *Can. J. Earth. Sci.* **20**, 1862-1879.

VON DREELE, R.B. (1997): Quantitative texture analysis by Rietveld refinement. *J. Appl. Crystallogr.* **30**, 517-525.

WARDLE, R. & BRINDLEY, G.W. (1972): The crystal structures of pyrophyllite, 1Tc, and of its dehydroxylate. *Am. Mineral.* **57**, 732-750.

WILLIAMS, P.P. & MEGAW, H.D. (1964): The crystal structures of low and high albites at –180°C. *Acta Crystallogr.* **17**, 882-890.

YOUNG, R.A. & POST, B. (1962): Electron density and thermal effects in alpha quartz. *Acta Crystallogr.* **15**, 337-346.

Received April 10, 2001, revised manuscript accepted November 9, 2001.